Solar System Research, Vol. 37, No. 1, 2003, pp. 31–35. Translated from Astronomicheskii Vestnik, Vol. 37, No. 1, 2003, pp. 34–39.

Space Weathering on Mercury: Implications for Remote Sensing*

S. K. Noble and C. M. Pieters
Brown University, Dept. of Geological Sciences, Providence RI 02912
e-mail: noble@porter.geo.brown.edu
Received February 22, 2002

Abstract—By applying our understanding of lunar space weathering processes, we can predict how space weathering will effect the soil properties on Mercury. In particular, the extreme temperature range on Mercury may result in latitudinal variations in the size distribution of $npFe_0$, and therefore the spectral properties of the soil.

INTRODUCTION

Space weathering processes are very important on the Moon. These processes both create the lunar regolith and alter its optical properties (Pieters *et al.*, 2000; Noble *et al.*, 2001; Hapke, 2001). Like the Moon, Mercury has no atmosphere to protect it from the harsh space environment and therefore it is expected that it will also incur the effects of space weathering (e.g. Hapke, 2001). However, there are many important differences between the environments of Mercury and the Moon. These environmental differences will almost certainly affect the weathering processes and the products of those processes. It should be possible to observe the effects of these differences in Vis/Nir spectra of the type expected to be returned by Messenger and Bepi Columbo, two upcoming missions which will explore Mercury (Solomon *et al.*, 2001; Grard and Mukai 2001). More importantly, understanding these weathering processes and their consequences is essential for evaluating the spectral data returned from these and other missions in order to determine the abundance of iron and the mineralogy of the Mercurian surface.

LESSONS FROM THE MOON

The lunar soil samples have provided a wonderful opportunity to study the effects of space weathering firsthand. “Space weathering” is an ill-defined phrase that is used to describe a number of processes that result in the space environment from the continuous bombardment of the surface by energetic cosmic and solar rays, solar wind particles, and micrometeorites. These processes occur on bodies that lack a substantial atmosphere. On the Moon, the constant flux of high energy particles and micrometeorites, along with larger meteorites, act to comminute, melt, sputter and vaporize components of the soil, as well as to garden (overturn) it. The products of these weathering processes include development of complex agglutinates as well as surface-correlated products on individual soil grains, such as: implanted rare gases, solar flare tracks, and a variety of accreted components. Recent detailed microanalytical studies (Keller *et al.*, 1998; Wentworth *et al.*, 1999) describe very thin (60–200 nm) patinas, or rims, of amorphous material developed on lunar soil grains (Fig. 1). The rims are created by both subtractive (radiation damage) and additive (vapor deposition and solar wind sputtering) processes.

The optical effects of space weathering are threefold (McCord and Adams, 1973; Fischer and Pieters, 1994). As lunar soils mature they (1) become darker (lower albedo), (2) lose their spectral contrast (the strength of the absorption bands are reduced) and (3) develop a characteristic continuum for which reflectance increases toward longer wavelengths.

Cassidy and Hapke (1975) first suggested that the continuum slope might be due to inclusions of nanophase iron ($npFe^0$). These tiny metallic iron particles are now known to be ubiquitous in the rim material (Keller *et al.*, 1999). In the lunar case, formation of $npFe^0$ in rims is largely created by vapor fractionation and sputtering of local FeO-bearing material. Neither process requires a H-saturated surface (Hapke, 2001). On the other hand, larger, but still sub-microscopic, Fe is also found throughout lunar agglutinates resulting from the reduction of FeO by interaction with solar wind H in a melt. The spheres of $npFe^0$ found in agglutinates are at least twice as large as those found in amorphous rims, averaging ~7 nm in diameter vs. ~3 nm for the rims (Keller and Clemett, 2001). A second study using backscattered election images suggests that the agglutinitic $npFe^0$ may be significantly larger yet, averaging over 100 nm in diameter (James *et al.*, 2001). The size distribution of metallic Fe particles in a soil strongly controls the effects on the Vis/Nir spectrum. It

*This article is based on the paper presented at the 34th International Microsymposium (Vernadskii–Brown) on Comparative Planetology (October 8–9, 2001).

0038-0946/03/3701-0031$25.00 © 2003 MAIK “Nauka / Interperiodica”

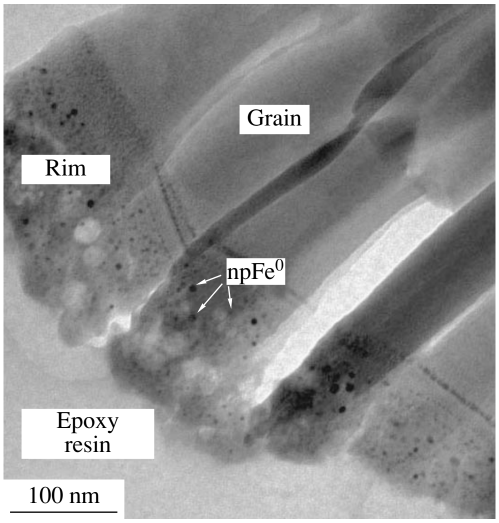

Fig. 1. TEM bright field image of a lunar soil grain with a complex weathered rim containing $npFe^0$.

appears that larger nanophase Fe^0 particles (those greater than ~10 nm in diameter) result in darkening of the soil (Keller *et al.*, 1998; Britt and Pieters, 1994); while the smaller particles (<5 nm in diameter) are largely responsible for the more complex continuum-altering effects.

MERCURIAN ENVIRONMENT

It will be a while before samples of Mercury's soil will be available to study, but by understanding the ways in which Mercury's environment differs from the Moon's, predictions can be made as to how space weathering will effect Mercury. Because of its proximity to the Sun, Mercury has a flux of impactors 5.5 times that of the Moon (Cintala, 1992). Also, its location in the solar system and greater mass require much faster velocity impacts. These factors combine to make Mercury much more efficient than the Moon at creating melt and vapor. Per unit area, impacts on Mercury are expected to produce 13.5 times the melt and 19.5 times the vapor than is produced on the Moon (Cintala, 1992). Mercury has a magnetic field that helps to protect its surface from charged particles, such that the solar wind flux at the surface is significantly less than in the lunar environment despite its proximity to the Sun (e.g., Hartle *et al.*, 1975; Killen *et al.*, 2001). The combination of these factors means that melting and vaporization due to micrometeorites will dominate space weathering on Mercury with little solar wind sputtering effects (Hapke, 2001). Furthermore, agglutinitic glass-like deposits and vapor deposited coatings should be created much faster and more efficiently on Mercury.

The nanometer-scale metallic Fe particles ($npFe^0$) that are ubiquitous in the rims and agglutinates of lunar soil (Keller and Clemett, 2001) should also be present on Mercury. Most predictions of Mercury's surface composition suggest that the surface is low in iron. Using microwave data, Jeanloz *et al.*, (1995) suggested that the surface of Mercury may have virtually no Fe^{2+}. McCord and Clark (1979) compared Vis/NIR reflectance spectra with lunar data and concluded that the amount of Fe^{2+} present should be similar to lunar highlands, roughly 6%. Recently, Hapke (2001) suggested that there should be about 3% FeO present based on the shape of the continuum. Even for the extreme endmember case where the surface of Mercury has no native FeO, the iron brought in by meteorites should be sufficient to make the formation of $npFe^0$ through vapor fractionation an important process on the planet. Lacking any large scale recycling mechanism (i.e., plate tectonics), meteoritic components should make up several percent of the regolith. From trace elements, iridium in particular, it has been estimated that 1–4% of the lunar soil is meteoritic contamination (Heiken *et al.*, 1991). If the Meteorite flux at Mercury is 5.5× greater (Cintala, 1992), the surface soils may contain as much as 5–20% meteoritic components. Iron brought in by meteorites could account for as much as 1–5% FeO in the regolith. Amounts as small as 0.05 wt % $npFe^0$ are enough to affect the optical properties (Noble *et al.*, 2001).

The Mercurian environment is also unique in our solar system because of its extreme temperature range. Due to its slow rotation and proximity to the Sun, equatorial regions of Mercury can achieve temperatures above 700 K during the day, while nighttime temperatures can dip below 100 K. These conditions will have important effects on diffusion in glass and crystal growth processes.

SPACE WEATHERING ON MERCURY

What, if any, effects might Mercury's unique environment have on space weathering products? The possibilities fall into two groups. (1) *Formation processes*: What weathering products are formed on Mercury and how do they compare to those on the Moon? (2) *Evolution processes*: How do the products of space weathering change as they are exposed to the Mercurian thermal regime?

Formation Processes

Melt products produced from micrometeorites that impact on the nightside of Mercury are expected to look similar to those observed in lunar soil. The major difference should be the rate of formation. As discussed above, agglutinitic glass and vapor should be forming at a much faster rate (Cintala, 1992). In a mature lunar soil, agglutinates make up as much as 50–60% of the soil. A mature soil on Mercury probably has little, if any, original crystalline material remaining. In addition, Mercurian agglutinates should contain less $npFe^0$ than their lunar counterparts assuming a lower initial amount of surface FeO available. Also, because the $npFe^0$ in lunar agglutinates is believed to be created

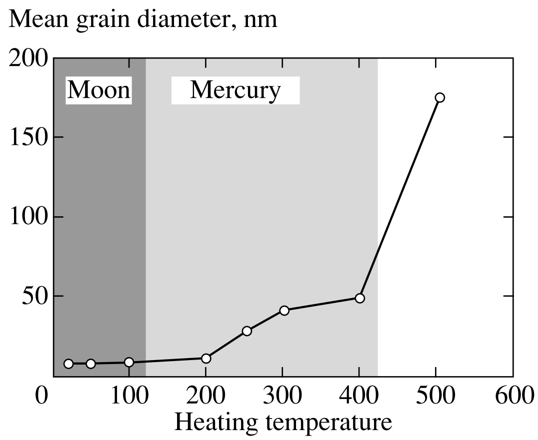

Fig. 2. Size of $npFe^0$ after annealing for 10 hours. Modified from Gleiter (1989). The shaded areas show the upper extent of the temperature regimes for the Moon and Mercury.

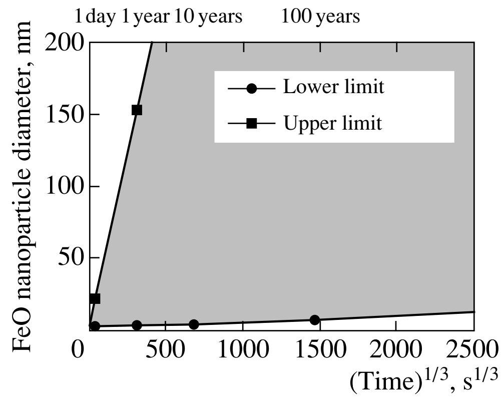

Fig. 3. Possible range of effects of Ostwald ripening with time near the equator of Mercury (based on equation 1). Lower bound assumes x_{IL} = 0.01, D = 10^{-19} m^2/s, σ = 0.1 mJ/m^2, Upper bound assumes x_{IL} = 0.1, D = 10^{-17} m^2/s, σ =100 mJ/m^2.

when the solar wind implanted H interacts with the melt to reduce FeO into Fe^0, its formation may be further limited on Mercury due to the reduced availability of solar wind.

Our calculations of cooling rates of spherical particles has shown that the extreme temperature range between night and day on Mercury will have only negligible effects on agglutinate formation. The increased heat during the day will allow longer cooling times for impacts into the day side vs. the night side. However, the cooling times for the formation of submillimeter melt particles will still be insufficient for full crystallization to occur. This diurnal effect would become more important for larger (~5–14mm diameter) melt bodies. Melt droplets in this size range would have sufficient time to crystallize during the day, but not at night. However, melt droplets in this size range would be orders of magnitude less common than agglutinate-sized particles.

Evolution processes

The thermal regime on Mercury may have significant effects on the $npFe^0$ in weathering products. Regardless of whether these melt and vapor products were created in the day or night, they will be exposed repeatedly to the extreme heat of Mercury's day.

Due to differences in free energy between curved surfaces, $npFe^0$ particles in a glass matrix will tend to coarsen via a process well known in material sciences, Ostwald ripening. Figure 2 shows the results of a $npFe^0$ study in which $npFe^0$ particles averaging about 8 nm in diameter were created and then heated for 10 hours at a range of temperatures. The graph plots the final size of the particles vs. the heating temperature. This study is not directly applicable to Mercury because they used only iron particles in grain to grain contact and not isolated iron particles suspended in a glass matrix. However, it is useful because it demonstrates that this size range of nanophase Fe particles is stable to about 200°C (Fig. 2), thus we should not expect Ostwald ripening to occur on the Moon, but the majority of Mercury's surface reaches daytime temperatures above 200°C. In fact, during the course of a Mercurian day, the soil at the hottest parts of Mercury will stay above 400°C for about 2 weeks. This increased temperature may be enough to allow the $npFe^0$ particles to grow significantly, at least near the equator. In a perhaps related experimental arrangement, a vapor deposition experiment of Hapke *et al.* (1994) demonstrated that heating $npFe^0$-rich vapor coatings to a temperature of 650°C for just one hour is sufficient to remove the ferromagnetic resonance. This presumably occurs because particles of $npFe^0$ have grown to be larger than the range that is measured by FMR techniques [4–33 nm in diameter (Housley *et al.*, 1976)] suggesting that the size of those particles tripled or quadrupled in the course of the experiment. Thus, it appears that even for $npFe^0$ particles suspended in a glass matrix increased temperatures can result in significant grain growth.

Determining the rate of Ostwald ripening on Mercury is difficult due to a lack of directly relevant experimental data. The equation for this process is given below along with estimates of values for each variable. The least constrained, and most important, variables are D, the diffusion coefficient which is strongly temperature dependent, and $npFe^0$, the surface energy (i.e., energy of boundary between $npFe^0$ and matrix) which is also temperature dependent. Considering a wide range of values for these, we have attempted to bound the possible range of grain growth through time. Figure 3 was calculated with following equation (Lifshitz and Slyozov, 1961):

$$r^3 - r_0^3 = \frac{8}{9}\frac{x_{IL}(1-x_{IL})}{(x_{IS}-x_{IL})^2}\frac{D\Omega\sigma}{RTI}(t-t_0), \qquad (1)$$

where r = original size of r_0 3 nm = 3×10^{-9} m (Keller and Clemett, 2001); x_{IL} = fraction of npFe^0 in rim coating = 0.1 (Hapke, 2001) - 0.01; x_{IS} = fraction of glass = 1; D = diffusion coef. of Fe in glass = 10^{-17}–10^{-19} m^2/s (Hoffman, 1980; Wang *et al.*, 1988); Ω = molar volume of Fe = 7.09×10^{-6} m^3/ mol; σ = surface energy = 0.1–100 mJ/m^2; T = 600 K; R = gas constant (R = 8.3143 J / mol K); I = thermodynamic factor ≈ 1; $t - t_0$ = time of exposure.

Even our most conservative estimates indicate that Ostwald ripening should have a significant effect on some Mercurian soils, doubling the size of the npFe^0 in a matter of centuries. Of course, with increasing latitude, there is less heat available and the thermal regime becomes much more lunar-like where Ostwald ripening will have little effect.

DISCUSSION

The size of npnpFe^0 particles will also be reflected in our remote datasets. Ostwald ripening should result in larger Fe particles, on average, near the equator. As noted earlier, small npFe^0 particles (<5 nm) cause reddening of the reflectance spectrum and larger ones result in darkening, if Ostwald ripening dominates over npFe^0 production, we expect the spectral continuum to be darkest near the equator and become somewhat redder with increasing latitude.

To date, none of the effects discussed above have been observed directly. Our current spectral data set for Mercury however, is very limited. Most of our spectral data is telescopic (Vilas, 1988), largely providing an integrated disk view, masking any possible latitudinal variations, as well as regional differences. Also hidden are maturity differences that might be expected at young craters. Two bands of spectral data taken during the Mariner 10 flyby confirms that spectral differences exist on regional and local scales (Robinson and Lucey, 1997), however this dataset does not have the spectral or spatial resolution necessary to see the effects discussed above. Recently, the surface was mapped over the wavelength range 550–940 nm at roughly 200 km resolution by the Swedish Vacuum Solar Telescope (Warell and Limaye, 2001). Unfortunately, latitudinal variations were removed in the calibration of this dataset.

FUTURE WORK

Much work needs to be done to constrain the rate of particle growth and to understand the temperature dependence of Ostwald ripening on npFe^0. In order to better constrain $D\sigma$, the diffusion coefficients of Fe in a glass matrix multiplied by the surface energy of the Fe, experiments must be preformed. We expect to utilize either a natural npFe^0-bearing material (e.g. lunar agglutinates) or an appropriate synthetically produced material with a known size distribution of npFe^0 particles to determine experimentally the rate of growth of npFe^0 with time. This information will allow us to calculate $D\sigma$ for the material, and thus substantially reduce the uncertainty in the size of this effect on Mercury.

CONCLUSIONS

Remote sensing methods generally do not sample the pristine rocks of the body, but rather the exposed regolith. Therefore, to get accurate results from remote datasets, the effects of soil formation and maturation processes (i.e. space weathering) on the properties of Mercury's soil must first be understood. The unique environment at Mercury, particularly its thermal regime is expected to have subtle, but important effects on the soil that will impact our remotely obtained data.

If the weathering environment on Mercury can be understood, than the space weathering products we can be predicted. By combining these predictions with an understanding of the optical effects of weathering gleaned from laboratory studies of lunar soil, we hope to estimate the total Fe on the surface of Mercury and to provide the necessary tools for evaluation of mineralogy for future missions.

ACKNOWLEDGMENTS

Thanks to Paul Hess for introducing us to the concept of Ostwald ripening and to Yan Liang for patiently explaining the process to me. NASA support (NAG5-4303) is gratefully acknowledged.

REFERENCES

Britt, D.T. and Pieters, C.M., Darkening on Black and Gas-Rich Ordinary Chondrites: The Spectral Effect of Opaque Morphology and Distribution, *Geochim. Cosmochim. Acta*, 1994, vol. 58, no. 18, pp. 3905–3919.

Cassidy, W. and Hapke, B., Effects of Darkening Processes on Surfaces of Airless Bodies, *Icarus*, 1975, vol. 25, pp. 371–383.

Cintala, M.J., Impact Induced Thermal Effects in the Lunar and Mercurian Regoliths, *J. Geophys. Res. E*, 1992, vol. 97, pp. 947–973.

Fischer, E.M. and Pieters, C.M., Remote Determination of Exposure Degree and Iron Concentration of Lunar Soil Using VIS-NIR Spectroscopic Methods, *Icarus*, 1994, vol. 111, pp. 375–488.

Gleiter, H., Nanocrystalline Materials, *Progress in Mat. Sci.*, 1989, vol. 33, pp. 223–315.

Grard, R. and Mukai, T., BepiCOLOMBO, an Interdisciplinary Mission to the Planet Mercury, in *Mercury: Space Environment, Surface, and Interior*, 2001, Abstract no. 8024.

Hapke, B., Cassidy, W, Wells, E., *et al.*, *Vapor Deposits in the Lunar Regolith: Discussions and Reply, Science*, 1994, vol. 264, pp. 1779–1780.

Hapke, B., Space Weathering from Mercury to the Asteroid Belt, *J. Geophys. Res. E*, 2001, vol. 106, pp. 10039–10073.

Hartle, R., Curtis, S.A., and Thomas, G.E., Mercury's Helium Exosphere, *J. Geophys. Res.*, 1975, vol. 80, pp. 3689–3693.

Heiken, G.H., Vaniman, D.T., and French, B.M., *The Lunar Sourcebook*, New York: Cambridge Univ. Press, 1991.

Hofmann A. W. Diffusion in Natural Silicate Melts: A Critical Review, in *Physics of Magmatic Processes*, Hargraves, R.B., Ed., Princeton: Princeton Univ. Press, 1980, pp. 385–417.

Housley, R.M., Cirlin, E.H., Goldberg, I.B., and Crowe, H., Ferromagnetic Resonance Studies of Lunar Core Stratigraphy, *Proc. 7th Lunar Sci. Conf.*, 1976, pp. 13–26.

James, C.L., Basu, A., Wentworth, S.J., and McKay, D.S., Grain Size Distribution of Fe^0 Globules in Lunar Agglutinitic Glass: First Results from *Apollo 17* Soil 78421, *GSA Annual Meeting*, 2001, Abstract no. 27433.

Jeanloz, R., Mitchell, D.L., Sprague, A.L., and de Pater, I., Evidence for a Basalt-Free Surface on Mercury and Implications for Internal Heat, *Science*, 1995, vol. 268, pp. 1455–1457.

Keller, L.P., Wentworth, S.J., and McKay, D.S., Surface Correlated Nanophase Iron Metal in Lunar Soils: Petrography and Space Weathering Effects, *New Views of the Moon*, 1998, Abstract no. 6033.

Keller, L.P., Wentworth, S.J., McKay, D.S., *et al.*, Space Weathering in the Fine Size Fractions of Lunar Soils: Soil Maturity Effects, *New Views of the Moon II*, 1999, no. 8052.

Keller, L.P and Clemett, S.J., Formation of Nanophase Iron in the Lunar Regolith, *Lunar Planet. Sci. Conf. XXXII*, 2001, 2097.

Killen, R.M., Potter, A.E., Reiff, P., *et al.*, Evidence for Space Weather at Mercury, *J. Geophys. Res. E*, 2001, vol. 106, no. 9, pp. 20509–20525.

Lifshitz, I.M., and Slyozov, V.V., The Kinetics of Precipitation from Supersaturated Solid Solutions, *J. Phys. Chem. Solids*, 1961, vol. 19, pp. 35–50.

McCord, T.B. and Adams, J.B., Progress in Remote Optical Analysis of Lunar Surface Composition, *The Moon*, 1973, vol. 7, pp. 453–474.

McCord, T.B. and Clark, R.N., The Mercury Soil: Presence of Fe^{2+}, *J. Geophys. Res.*, 1979, vol. 84, pp. 7664–7668.

Noble, S.K., Pieters, C.M., Taylor, L.A., *et al.*, The Optical Properties of the Finest Fraction of Lunar Soil: Implications for Space Weathering, *Meteoritics Planet. Sci.*, 2001, vol. 36, pp. 31–42.

Pieters, C.M., Taylor, L.,A., Noble, S.K., *et al.*, Space Weathering on Airless Bodies: Resolving a Mystery with Lunar Samples, *Meteoritics Planet. Sci.*, 2000, vol. 35, pp. 1101–1107.

Robinson, M.S. and Lucey, P.G., Recalibrated *Mariner 10* Color Mosaics: Implications for Mercurian Volcanism, *Science*, 1997, vol. 275, pp. 197–199.

Solomon, S.C., McNutt, R.L. Jr., Gold R. E., *et al.*, The *MESSENGER* Mission to Mercury, in *Mercury: Space Environment, Surface, and Interior*, 2001, 8030.

Vilas, F., Surface Composition of Mercury from Reflectance Spectrophotometry, in *Mercury*, Tucson: Univ. of Arizona Press, 1988, pp. 59–76.

Wang, P.W., Feng, Y.P., Roth, W.L., and Corbett, J.W., Diffusion Behavior of Implanted Iron in Fused Silica Glass, *J. Non-Cryst. Solids*, 1988, vol. 104, pp. 81–84.

Warell, J. and Limaye, S.S., Properties of the Hermian Regolith: I. Global Regolith Albedo Variation at 200 km Scale from Multicolor CCD Imaging, *Planet. Space Sci.*, 2001 (in press).

Wentworth, S.J., Keller, L.P., McKay, D.S., and Morris, R.V., Space Weathering on the Moon: Patina on *Apollo 17* Samples 75 075 and 76 015, *Meteoritics Planet. Sci.*, 1999, vol. 34, pp. 593–603.